Available online at www.sciencedirect.com
SCIENCE DIRECT
Polymer 46 (2005) 9664–9673
polymer
www.elsevier.com/locate/polymer

Fabrication and characterization of microgel-impregnated, thermosensitive PNIPAAm hydrogels

Xian-Zheng Zhang[a,b], Chih-Chang Chu[b,*]

[a]Key Laboratory of Biomedical Polymers of Ministry of Education, Department of Chemistry, Wuhan University, Wuhan 430072, People's Republic of China
[b]Department of Textiles and Apparel and Biomedical Engineering Program, Cornell University, Ithaca, NY 14853-4401, USA

Received 24 June 2005; received in revised form 9 August 2005; accepted 17 August 2005
Available online 6 September 2005

Abstract

Poly(*N*-isopropylacrylamide)/poly(ethylene glycol) diacrylate (PNIPAAm/PEG-DA) microgels were used as an additive during the polymerization and/or crosslinking of PNIPAAm hydrogels to improve their thermosensitive properties. The influence of this additive on the property of resulting PNIPAAm hydrogels was investigated and characterized. The interior morphology by scanning electron microscopy (SEM) revealed that microgel impregnated PNIPAAm hydrogels have tighter and constrained porous network structures, although large cavities of 30–40 μm in diameter, occupied by the microgels were sporadically distributed in this constrained network. Differential scanning calorimetry (DSC) studies did not show apparent difference in lower critical solution temperature (LCST) between normal and microgel-impregnated PNIPAAm hydrogels. The incorporating of PNIPAAm/PEG-DA microgels, however, significantly improved mechanical properties of modified hydrogels when comparing with a normal PNIPAAm hydrogel, although the tendency was not strictly proportional to the microgel amount. Based on the temperature-induced swelling ratio data as well as response kinetics, microgel-impregnated hydrogels exhibited improved thermosensitive characteristics in terms of higher equilibrium swelling ratio as well as faster response rates and the level of improvement depended on the amount of microgel impregnated.

Keywords: Microgel; Poly(*N*-isopropylacrylamide) hydrogel; Poly(ethylene glycol)

1. Introduction

A signal-triggered phase separation of hydrogels has attracted extensive research interest recently. Sharp physical changes of hydrogels are triggered by various external stimuli; as a result, these hydrogels could undergo a reversible discontinuous phase transition [1–4]. Among those external stimuli, temperature is an important triggering signal for phase transitions in hydrogels, and poly(*N*-isopropylacrylamide) (PNIPAAm) hydrogel is the best known thermosensitive polymeric network, which exhibits a transition temperature (T_{tr}) or lower critical solution temperature (LCST) at about 33 °C [5,6]. At a temperature above LCST, the hydrogen-bonding efficiency becomes weaker for proper solubility of PNIPAAm in water. As a result, a thermoreversible phase separation occurs and a polymer-enriched phase and an aqueous phase that contains nearly no polymer form. Due to this unique property, PNIPAAm hydrogel has been widely studied for biomedical uses including as the carrier matrix for controlled drug release, protein–ligand recognition, and immobilization of enzyme [7–9].

A drawback of normal PNIPAAm hydrogels is their slow response behavior to an applied signal. It is known that the purpose of controlled release of drugs is to improve their therapeutic value by reducing toxic side effects of drugs. When a PNIPAAm hydrogel was used as a drug carrier for controlled release, due to its inherent temperature-triggering capability, the amounts of drug released may be self-monitored. This release pattern was generally recognized as an on–off switching release of drugs [10]. With a fast response to temperature stimuli, the solute (i.e. drug) might release from the improved hydrogel quickly, and such a kind of drug release would present a much better on–off switching release pattern than using a normal hydrogel with a slower response rate. In addition, in some other

* Corresponding author. Tel.: +1 607 255 1938; fax: +1 607 255 1093.
E-mail address: cc62@cornell.edu (C.-C. Chu).

0032-3861/$ - see front matter © 2005 Elsevier Ltd. All rights reserved.
doi:10.1016/j.polymer.2005.08.055

occasions, such as artificial organs [11] and actuators [12], the improved response rate is also a crucial factor to improve practical application of such an intelligent biomaterial.

There are several approaches that have been proposed to improve the response rate for such hydrogels via either the change of chemical and/or physical structures. One of approaches is the porosigen technique which involves the use of pore-forming agents, such as sodium chloride [13] and sucrose [14]. During the gelation process, due to the existence of the pore-forming agent, the resulting network matrix may be macroporous. For an instance, Wu et al. [15] reported the preparation of macroporous hydrogels by using hydroxypropyl cellulose (M_W 300,000) as a pore-forming agent. Such a macroporous hydrogel responds to temperature changes much faster than hydrogels prepared by a conventional method (i.e. without using pore-forming agents). However, the polymerization temperature they employed was above LCST and the macroporous hydrogel has a heterogenerous microstructure. It was possible that the heterogeneity in structure may also be responsible for the macroporosity of the modified hydrogels.

Recently, poly(ethylene glycol) (PEG) was used as a promising pore-forming agent to obtain a macroporous PNIPAAm hydrogel [16,17] because of the fact that poly(ethylene glycol) (PEG) exhibits a spherical shape in solution [18]. The polymerization of *N*-isopropylacrylamide (NIPAAm) was carried out at room temperature and the resulted PNIPAAm hydrogels have a homogenerous structure. It was found that if the molecular weight of PEG was <2000, the pore size was a dominant factor that increased the response rate of PNIPAAm hydrogels. However, when a much higher molecular weight PEG was used, the response rate might be reduced slightly, although the modified hydrogel retained its macroporous morphology.

A new approach of using thermo-responsive microgels as additives to improve the response rate of PNIPAAm hydrogel was reported by Cai and Gupta in their study of using poly(*N*-isopropylacrylamide-*co*-acrylic acid) microgel particles as additives to prepare fast responsive bulk hydrogels, which exhibited improved swelling capability [19]. The main advantage of this new approach is that the microgel additives incorporated have thermo-responsive capability as surrounding matrices.

In this paper, we advanced the microgel additive concept further by using microgels consisted of a copolymer of PNIPAAm and poly(ethylene glycol) diacrylate (PEG-DA); and these microgels were used as new pore-forming additives to prepare faster response PNIPAAm hydrogels with significant improvement in mechanical property. The morphological, thermal, and mechanical properties of the microgel-impregnated PNIPAAm hydrogels were characterized by scanning electron microscopy (SEM), differential scanning calorimetry (DSC), and compression modulus measurements. The temperature dependence of the swelling ratio, response kinetics upon heating or cooling, and oscillatory shrinking–swelling kinetics over temperature cycles around LCST of the microgel-impregnated PNIPAAm hydrogels were further examined to assess the influence of the microgel additive on thermosensitive capability of PNIPAAm hydrogels.

2. Experimental Part

2.1. Materials

N-isopropylacrylamide (Aldrich Chemical, USA) was further purified by recrystallization in benzene/*n*-hexane. Dextran of molecular weight 66,000, Poly(ethylene glycol) diol of molecular weight 8000, acryloyl chloride, *N*,*N*′-methylenebisacrylamide (MBAAm), anhydrous magnesium sulfate ($MgSO_4$), ammonium persulfate (APS) and *N*,*N*,*N*′,*N*′-tetramethylethylenediamine (TEMED) were purchased from Sigma Chemical (St Louis, Missouri, USA) and used as supplied.

2.2. Synthesis of PNIPAAm/PEG-DA microgel

PNIPAAm/PEG-DA microgel was prepared according to our previous work [20,21] in the aqueous two-phase system. In brief, PEG-DA of M_W 8000 was synthesized and purified according to Cruise et al. published procedures [22], This PEG-DA precursor and NIPAAm monomers were dissolved in distilled water to form an aqueous phase. Then, Dextran 66,000 and anhydrous $MgSO_4$ were dissolved in distilled water to form another aqueous phase. The above two aqueous solutions were vigorously mixed at a stirring rate of 800 rpm. Phase separation took place and the resulting water-in-water emulsion system was allowed to stabilize for 30 min. APS and TEMED were subsequently added to initiate the polymerization of NIPAAm monomers as well as the crosslinking of acryloyl moieties in the NIPAAm and PEG-DA for 12 h at room temperature (22 °C) without stirring. The crosslinked PNIPAAm/PEG-DA microgels were purified by multiple centrifugation and washing steps with distilled water and were then freeze-dried in a Virtis Freeze Drier (Gardiner, NY) under vacuum at −42 °C for 3 days for following studies.

2.3. Fabrication of microgel impregnated PNIPAAm hydrogels

The microgel-impregnated PNIPAAm hydrogels were prepared by incorporating various amounts of PNIPAAm/PEG-DA microgels into the aqueous solution of NIPAAm precursor in a glass bottle of 25 mm internal diameter and 45 mm in height with the presence of MBAAm crosslinker. First, microgels were immersed and dispersed in distilled water by reaching the swollen state of microgels. Then, NIPAAm precursor, MBAAm crosslinker and APS initiator

were added into the solution of microgel. After stirring well at room temperature, TEMED were subsequently added into the mixture solution and the reaction glass bottle was sealed for carrying out the copolymerization/crosslinking reactions for 90 min. The resulting microgel-impregnated PNIPAAm hydrogels were designated as Gel_x, where x indicated the microgel feed amount during the hydrogel fabrication. Normal PNIPAAm hydrogel (NG) was prepared in the same manner, except in the absence of microgels and NG was used as the control. All samples prepared above were washed with distilled water at room temperature and distilled water was replaced with fresh one every several hours to remove any unreacted chemicals within the hydrogel matrix. The washed hydrogels were cut into disc-shape pieces of approximately 10 mm in diameter and 4 mm in thickness for characterization studies. The feed composition and fabrication conditions of hydrogels are summarized in Table 1.

2.4. SEM observation of interior morphologies

The hydrogel samples were first equilibrated in distilled water at room temperature to reach an equilibrium state and the swollen, equilibrated hydrogel samples were quickly frozen in liquid nitrogen and further freeze-dried under vacuum at −42 °C for 3 days until the solvent was sublimed. The freeze-dried hydrogels were then fractured carefully and the interior morphology of the hydrogels was studied by using a scanning electron microscope (Hitachi S4500 SEM, Mountain View, CA). Before SEM observation, hydrogel specimens were fixed on aluminum stubs and coated with gold for 40 s under vacuum.

2.5. LCST behaviors

The LCST behavior of hydrogel samples was determined using a Perkin–Elmer 7-Series differential scanning calorimeter (DSC, Model DSC 4, Perkin–Elmer Cetus Instruments, Norwalk, CT). All samples were immersed in distilled water at room temperature and allowed to swell to reach the equilibrium state before DSC measurement. The swollen sample along with its water was placed in a hermetic sample pan and sealed. Thermal analyses were performed on swollen samples from 25 to 50 °C at a heating rate 3 °C/min under a dry nitrogen atmosphere (flow rate of 40 mL/min).

2.6. Mechanical properties

The mechanical properties of swollen hydrogel samples were measured by an Instron model 1122 (Instron Corporation, Canton, Massachusetts, USA) at 22 °C and 63% relative humidity with a compression load cell having a full-scale range of 2.0 KN. Before mechanical property experiment, all samples were immersed in water at room temperature for 2 days to reach their equilibrium swollen state, the swollen hydrogel was then placed on the top plate of a compression load cell and compressed by a cylindrical shaped metal rod probe (diameter 6 mm) at a constant crosshead speed of 0.5 mm/min until fragmentation of the hydrogel was occurred. The thickness of the hydrogel was evaluated using a compressometer (Frazier Instruments, Hagerstown, MD). Initial compression modulus was calculated from the initial slope of the stress–strain curve and was used to represent the hydrogel mechanical property. The average value of two measurements for each sample was taken.

2.7. Temperature dependence of swelling ratios

For the temperature-induced swelling study, hydrogels were equilibrated in distilled water at a temperature ranging from 22 to 50 °C. The samples were allowed to swell in distilled water for at least 24 h at each predetermined temperature controlled up to ±0.1 °C by a thermostated water bath (Grant Precision Stirred Bath, Grant Instruments Ltd, Cambridge, England). The gravimetric method was employed to study the hydrogel's swelling ratio. After immersion in distilled water at a predetermined temperature, the hydrogels were removed from water bath and blotted with a wet filter paper to remove excess water on the hydrogel surface and then weighted until constant weight was reached. After this weight measurement, the hydrogel was re-equilibrated in distilled water at another

Table 1
Feed compositions and fabrication conditions of microgel-impregnated PNIPAAm hydrogels

	Hydrogel samples[a]					
	NG	Gel_5	Gel_{10}	Gel_{20}	Gel_{30}	Gel_{40}
NIPAAm (mg)	100	100	100	100	100	100
MBAAm (mg)	2	2	2	2	2	2
Microgel (mg)	0	5	10	20	30	40
H_2O (ml)	1.5	1.5	1.5	1.5	1.5	1.5
APS (mg)	3	3	3	3	3	3
TEMED (ml)	0.05	0.05	0.05	0.05	0.05	0.05
Conversion (%)[b]	91.2	87.8	86.4	82.2	79.8	67.4

[a] All reactions were carried out for 90 min at room temperature in distilled water.
[b] Weight percentage of the synthesized hydrogel from the precursor, NIPAAm.

predetermined temperature and its wet weight was determined thereafter. The dry weight of each sample was determined after drying to constant weight under vacuum at 60 °C for overnight. The average values among three measurements were taken for each sample, and the swelling ratio was calculated as follows,

$$\text{Swelling ratio} = \frac{W_s - W_d}{W_d} \quad (1)$$

where W_s was the weight of the wet hydrogel after reaching equilibrium at each predetermined temperature and W_d is the dry weight of hydrogel.

2.8. Deswelling or shrinking kinetics

The shrinking kinetics of the PNIPAAm hydrogels was measured gravimetrically at 48 °C which was well above the LCST of the PNIPAAm hydrogels so that dramatic shrinkage in volume or discontinuous phase separation could be attained within a short time. The hydrogel samples were first immersed in distilled water at room temperature till it reached equilibrium. The equilibrated hydrogel samples were then quickly transferred into a water bath at a temperature of 48 °C. At predetermined interval, the samples were removed from the hot water bath and weighted after wiping off the excess water on surface with a wet filter paper. Water retention was defined as follows:

$$\text{Water retention} = \frac{W_t - W_d}{W_e - W_d} \times 100 \quad (2)$$

where W_t is the weight of the wet hydrogel at time t and 48 °C, W_e is the weight of the hydrogel at equilibrated swelling at 22 °C, and W_d is the dry weight of hydrogel. Please be noted, at time $t=0$, $W_0 = W_e$.

2.9. Swelling kinetics

The swollen hydrogel samples were first immersed into hot water bath (48 °C) for about 2 h, and then the partly shrunk hydrogels were further dried in a vacuum oven at 55 °C overnight till the hydrogel reached constant weight. The dried samples were immersed in distilled water at 22 °C and removed from water at regular time intervals. After wiping off the water on the surfaces of the samples with wet filter papers, the weights of hydrogels were recorded and the water uptake is defined as follows:

$$\text{Water uptake} = \frac{W_t - W_d}{W_e - W_d} \times 100 \quad (3)$$

where W_t is the weight of the wet hydrogel at time t and 22 °C, W_e is the weight of the hydrogel at equilibrated swelling at 22 °C, and W_d is the dry weight of hydrogel. Obviously, at time $t = \infty$, $W_\infty = W_e$.

2.10. Oscillatory shrinking–swelling kinetics over temperature cycles

The deswelling studies may provide us with information about the influence of microgels incorporated on the deswelling rate of hydrogels. However, from the standpoint of applications, the oscillating shrinking–swelling properties to the small temperature cycles (e.g. cycled around the physiologic temperature) of the hydrogel is of importance. For this purpose, the temperatures operated in oscillatory swelling/deswelling are different to the temperature for

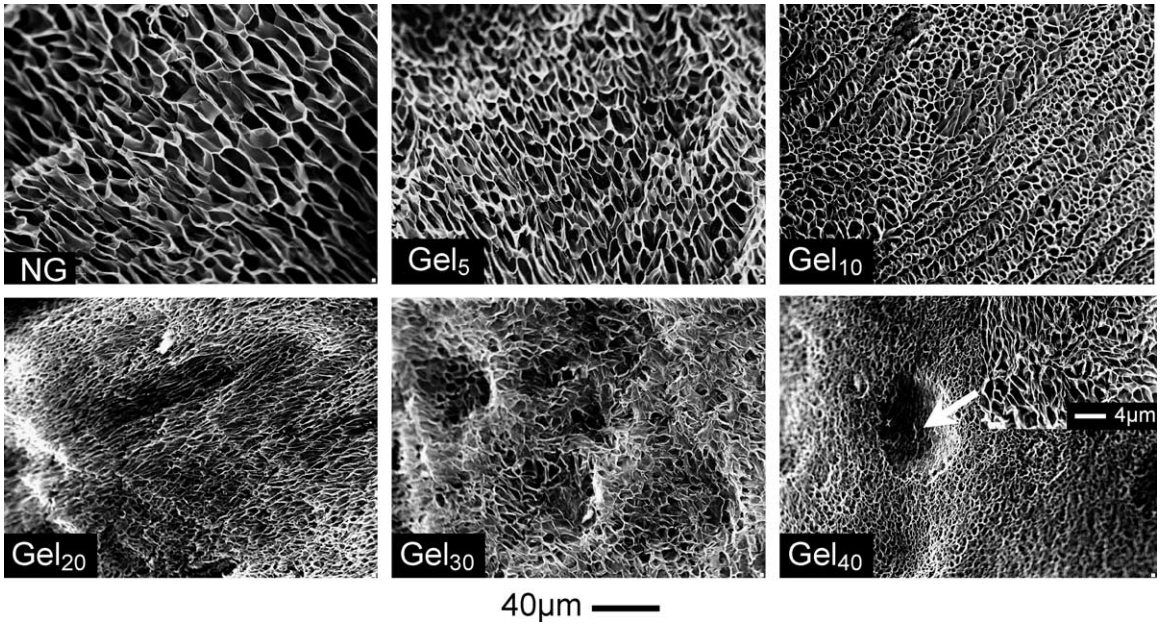

Fig. 1. Micrographs of freeze-dried, microgel-impregnated PNIPAAm hydrogels (all hydrogel samples were immersed into water for 2 days at room temperature before freezing-drying).

deswelling investigation. Here, the oscillatory shrinking–swelling kinetics of the hydrogels over the 6-min temperature cycles between 22 (below LCST) and 37 °C (above LCST) in distilled water were further investigated for determining the response rate of the microgel-impregnated PNIPAAm hydrogels upon temperature cycling. The hydrogel samples were first immersed in distilled water at 22 °C till it reached equilibrium. The hydrogel sample was then quickly transferred to distilled water at 37 °C and the sample exhibited shrinking behavior. After 3 min, the sample was taken out of the 37 °C water bath and its wet weight after blotting the excess water on the hydrogel surface by a wet filter paper was weighted and recorded. The sample was then transferred back to 22 °C distilled water for another 3-min swelling and weighted. This 6-min cycle (3 min for shrinking from 22 to 37 °C and 3 min for swelling from 37 to 22 °C) was continued for several cycles in order to determine the oscillatory shrinking–swelling kinetics of the hydrogels.

3. Results and discussion

3.1. Interior morphology

The interior morphology of microgel-impregnated PNIPAAm hydrogels is shown in Fig. 1. To our surprise, these PNIPAAm hydrogels (Gel_5–Gel_{40}) did not exhibit a macroporous network structure as observed by using conventional pore-forming agents like PEG (Fig. 2) [16]. Instead, they showed constrained and tighter porous network structure when compared with NG, and the level of tightness increased with an increase in the amount of PNIPAAm/PEG-DA microgel (from Gel_5 to Gel_{40}). Among all the hydrogels, the control (NG) had the largest pore size with an average 10 ± 5 μm in diameter. The pore size of the microgel-impregnated PNIPAAm hydrogels are smaller than the control and decreased with an increase in the content of the impregnated microgels, i.e. 7 ± 3 and 2 ± 1 μm in diameter for Gel_5 and Gel_{40}, respectively. Fig. 3 schematically shows the difference in network structures of the normal PNIPAAm hydrogel (a) and modified PNIPAAm hydrogel with a microgel additive.

The dependence of gelation level (indicated by the conversion (%) in Table 1) of PNIPAAm hydrogels on the amounts of impregnated microgels is probably attributed to the large physical size of the impregnated PNIPAAm/PEG-DA microgels as these microgels are much larger than the conventional pore-forming agents like PEG. The average diameter of spherical shaped PEGs of different molecular weight was reported to be very small [23], while the hydration diameter of the PNIPAAm/PEG-DA microgel used in this study is around 50 μm [20,21]. During the polymerization/crosslinking processes, owing to the presence of large size microgels, it would be difficult for PNIPAAm gelation to take place, especial in the regions occupied by microgels. This reduced gelation level was further confirmed by the precursor to hydrogel conversion level as shown in Table 1 in which Gel_{40} had only 67.4% conversation, while the NG had 91.2%. We suggest that hydration and hence exclusion volume of microgels may provide macroscopic steric hindrance during the polymerization and/or crosslinking process; thus an increase in the amounts of microgels would lead to a lower level of gelation.

Another distinctive morphology in the microgel-impregnated PNIPAAm hydrogels is the presence of sporadically distributed large spherically-shaped impressions in the hydrogel matrix when the microgel to NIPAAm feed ratio went beyond 1:10 (Gel_{20}, Gel_{30} and Gel_{40}). In fact, these spherically-shaped impressions were the direct evidences of the existence of microgels within the hydrogel matrix. The diameter of the impression was from 30–40 μm (e.g. Gel_{40}), which agreed with the hydration diameter of the microgel [20,21]. The impressions observed on SEM images (Fig. 1) were from those microgels that were lost during sample preparation, such as the process of fracturing frozen specimens for revealing the interior as well as gold sputter coating under vacuum.

3.2. LCST behavior

Fig. 4 exhibits the LCSTs of normal and microgel impregnated PNIPAAm hydrogels. Virtually, all the hydrogels show a similar LCST around 35.5 °C. The onset point of the endothermal peak, determined by the

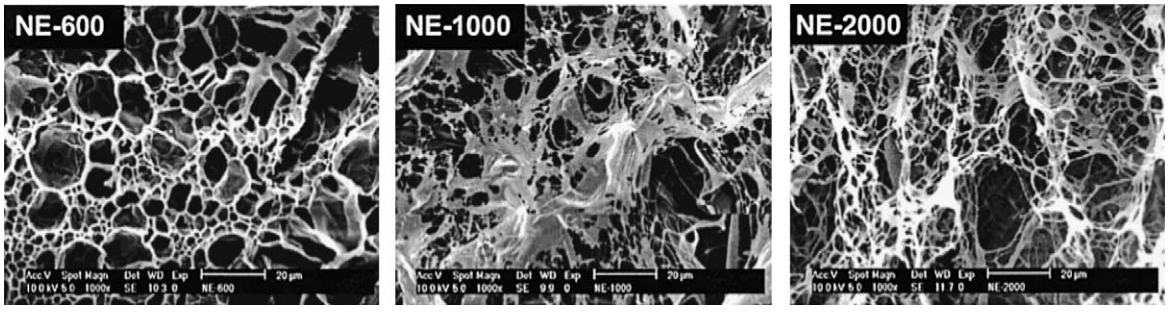

Fig. 2. SEM micrographs of the conventional and PEG-modified PNIPAAm hydrogels. The size of the bar is 20 μm (Ref. [16]).

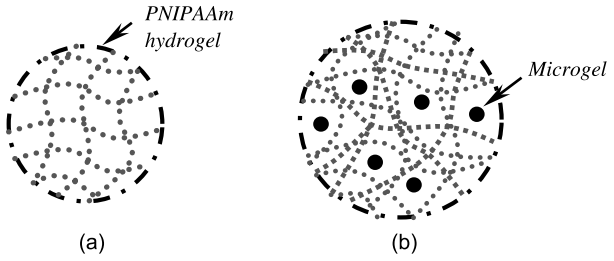

Fig. 3. Schematic illustration of network structures of (a) the normal PNIPAAm hydrogel and (b) microgel-impregnated PNIPAAm hydrogel.

intersecting point of two tangent lines from the baseline and slope of the endothermic peak, was used to determine LCST [24,25]. For instance, the LCST for the NG and Gel_{40} hydrogel are 35.8 and 35.3 °C, respectively. Thus, the presence of PNIPAAm/PEG-DA microgel additives did not change the LCST of the host PNIPAAm hydrogels.

In a PNIPAAm network system, there is a hydrophilic/hydrophobic balance [26–28] as well as many inter- and intramolecular interactions, such as hydrogen bonds and polymer–polymer interactions. These interactions lead to good swelling of the PNIPAAm hydrogel in water at room temperature (below LCST). The transition from hydrophilic (below LCST) to hydrophobic (above LCST) through heating is due to the breakage of hydrogen bonds in PNIPAAm chains. At a temperature above LCST, hydrogen bonds are destroyed and consequently PNIPAAm hydrogels become much less hydrophilic, which favors the hydrophobic interaction among PNIPAAm chains. At this stage, PNIPAAm chains precipitate from the water and the hydrogel structure collapses in volume, i.e. a phase separation from the aqueous medium. Since the PNIPAAm/PEG-DA microgel additive did not react with any precursors, i.e. NIPAAm and MBAAm during the gelation process, the resulted PNIPAAm hydrogel would have almost the same chemical structure as pure PNIPAAm (without the presence of microgels). The hydrophilic/hydrophobic balance would remain almost the same, thus the LCST did not change significantly, which also agrees with our previous findings [29].

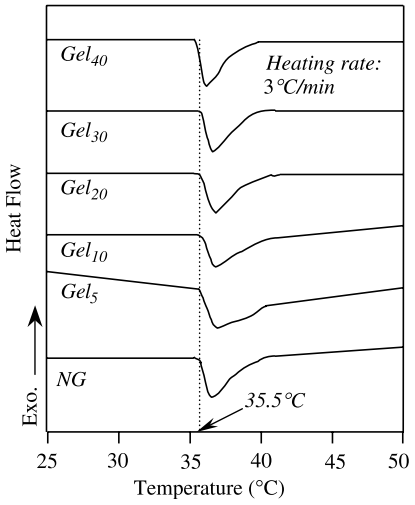

Fig. 4. DSC traces of swollen microgel-impregnated PNIPAAm hydrogels for determining their LCST (the onset temperatures of endotherms were referred as LCST).

3.3. Mechanical properties

The mechanical property, i.e. initial compression modulus of swollen PNIPAAm hydrogels, as a function of the weight percentage of impregnated PNIPAAm/PEG-DA microgels is shown in Fig. 5. The data revealed that the compression moduli of the microgel-impregnated PNIPAAm hydrogels were significantly greater than the normal PNIPAAm hydrogel (NG). Among the microgel-impregnated hydrogels, the increased compressive moduli, however, was not strictly proportional to the amounts of microgel additives. The compression modulus of Gel_5 increased to 24 KPa from 12.7 KPa of upon 5 mg microgel incorporation. With additional 5 mg microgels, the modulus of Gel_{10}, however, decreased to around 20 KPa from Gel_5. The compressive moduli reached a maximum of 34 KPa (Gel_{30}) and then decreased again to 25 KPa for Gel_{40}.

This overall higher mechanical property of the microgel-impregnated PNIPAAm hydrogels than NG is believed to be the result of both the reinforced effect of the microgels and the tighter and denser network structure of the surrounding PNIPAAm formed. As shown in the SEM morphology (Fig. 1), this tighter and denser network structure observed in all microgel-impregnated PNIPAAm hydrogels could increase the polymer mass per unit volume, i.e. increasing compressive modulus. The non-uniform increase in compressive modulus with the amounts of incorporated microgels may be attributed to the fact of poor interfacial bonding between the microgel additives and their surrounding PNIPAAm matrix. Such a poor interfacial bonding was evident from the presence of spherically-shaped void spaces

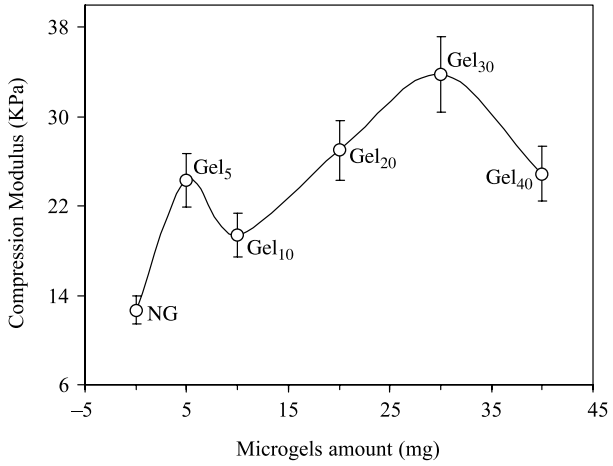

Fig. 5. Initial compression moduli of microgel-impregnated PNIPAAm hydrogels as a function of the amounts of impregnated PNIPAAm/PEG-DA microgels.

(Fig. 1) due to the relative ease of loss of these microgel spheres upon manipulation. This poor interfacial bonding also indicates that PNIPAAm/PEG-DA microgels did not chemically participate in the polymerization/crosslinking reaction of the surrounding NIPAAm monomers during the formation of the surrounding PNIPAAm matrix. In addition, if the amount of impregnated microgels was too high like in Gel_{40}, the continuity of the surrounding network structure could be interrupted and the mechanical property of interrupted network would be reduced as observed in the case of Gel_{40}.

The achievement of mechanically stronger hydrogels is important for their potential applications. For example, in some applications, an obvious limitation of a normal hydrogel is its poor mechanical property if used as the drug delivery device in a highly swollen state. Because of its non-biodegradable nature, surgical removal after drug release is desirable. If the device was too fragile and easily to be fragmented upon handling, it would be difficult to be completely removed through the traditional surgical procedures. Improving mechanical property of PNIPAAm hydrogels is also of particularly important for those applications requiring a faster response rate. It was known that the use of either phase separation at high temperatures [15] or pore-forming agents [16,17] could lead to fast responsive, macroporous PNIPAAm hydrogels. Due to the reduced polymer mass per unit volume from their macroporous networks, however, the mechanical property of the resulting hydrogels become very poor. While, in this study, we not only improved the mechanical property of PNIPAAm hydrogels by several folds, but also increased their response rate as given below.

3.4. Temperature dependence of swelling ratios

Fig. 6 shows the classical temperature-dependent swelling ratios of normal and microgel-impregnated PNIPAAm hydrogels over 22–50 °C, which covers the LCST of PNIPAAm hydrogels. The swelling data show that not only the swelling ratios of microgel-impregnated PNIPAAm hydrogels at room temperature were higher than that of normal PNIPAAm hydrogel but also the former had a much higher magnitude of swelling ratio reduction at their LCST than the normal hydrogel. For example, the swelling ratio of Gel_{40} (~70) is about 1.5 times of the one of NG (~47) at room temperature. A higher amount of the impregnated microgels within PNIPAAm matrix also led to a higher swelling ratio and larger deswelling degree.

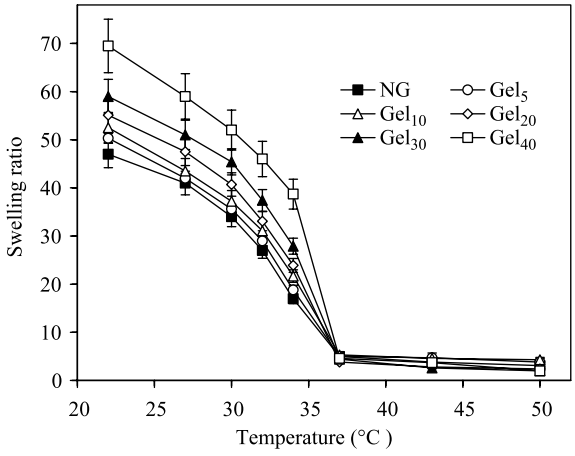

Fig. 6. Temperature dependence of swelling ratio of microgel-impregnated PNIPAAm hydrogels over the temperature range from 22 to 50 °C.

This dependence of swelling ratio on the amounts of the impregnated microgels within PNIPAAm matrix appeared to be related to the special morphological structure observed (Fig. 1). Generally, as a result of reduced pore size from NG to Gel_5 to Gel_{40}, the free volume within these hydrogel networks should be expected to be lower and hence lesser water should be accommodated, i.e. lower swelling ratio. However, the data in Fig. 6 indicate the opposite. The possible reason may be related to the presence of microgels, which possess temperature-induced swelling capability to provide additional three-dimensional porous network structure as the reservoir within the PNIPAAm matrix for water accommodation. As more of these microgels were impregnated into PNIPAAm matrix as from Gel_5 to Gel_{40}, more extra reservoir would be available for water accommodation, i.e. increasing swelling ratio from Gel_5 to Gel_{40} as observed.

The data in Fig. 6 also exhibit that all microgel-impregnated PNIPAAm hydrogels had similar temperature-dependence as normal PNIPAAm hydrogel did and reached similar final swelling ratios at temperatures above LCST. But the magnitudes of the thermo-induced swelling ratio change of microgel-impregnated PNIPAAm hydrogels were larger than NG which had Δswelling 44 ($=SR_{22\,°C}-SR_{5\,°C}$). Among microgel-impregnated PNIPAAm hydrogels, the Gel_{40} had the largest change in swelling ratio (Δswelling $=68$) upon temperature-induced deswelling, while Gel_5 had the smallest change (Δswelling $=47$). The possible reason for the relatively larger magnitude of temperature-induced deswelling ratio change in all microgel impregnated PNIPAAm hydrogels than the normal one may be also attributed to their microstructure difference as discussed above as the impregnated-microgels within PNIPAAm matrix would enhance the temperature-induced deswelling due to their inherent thermo-responsive capability.

The deswelling data in Fig. 6 also confirm that, irrespective of normal or microgel-impregnated hydrogels, the phase transition temperature (LCST) of these hydrogels (~35.5 °C) is in agreement with the LCST obtained from DSC measurement described previously.

3.5. Shrinking kinetics

Fig. 7 presents the shrinking kinetics of the normal and microgel impregnated PNIPAAm hydrogels after

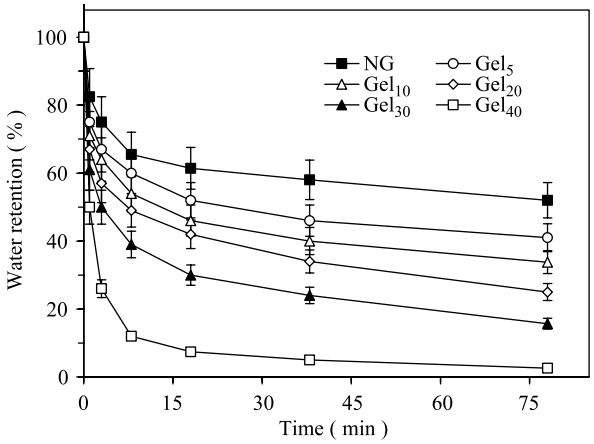

Fig. 7. Temperature response kinetics of microgel-impregnated PNIPAAm hydrogels at 48 °C.

transferring the equilibrated swollen specimens at 22 °C (below LCST) to hot water at 48 °C (above LCST). The microgel impregnated PNIPAAm hydrogels responded to the temperature increase much faster than NG. For example, after 18 min in 48 °C, Gel_{40} shrank dramatically and lost over 90% water. In contrast, only about 38% water was evacuated from NG within the same time frame. After 78 min, over 95% water was lost in Gel_{40} and it reached stable water content, whereas only about 50% water was lost from NG within the same time frame. Those Gel_5, Gel_{10}, Gel_{20}, Gel_{30} had 60, 66, 75, 82% water loss within 78 min. Among the microgel-impregnated PNIPAAm hydrogels, the shrinking rate also depended on the amount of microgel impregnated and the shrinking rate tended to accelerate from Gel_5 and Gel_{40} with an increase in microgel amount.

In our previous paper [30], it was suggested several factors that determine the response rate of PNIPAAm hydrogel at a temperature above LCST. The first factor is the shrinking desire. The microgel-impregnated PNIPAAm hydrogels would have the similar shrinking desire as the normal PNIPAAm hydrogel since they were virtually

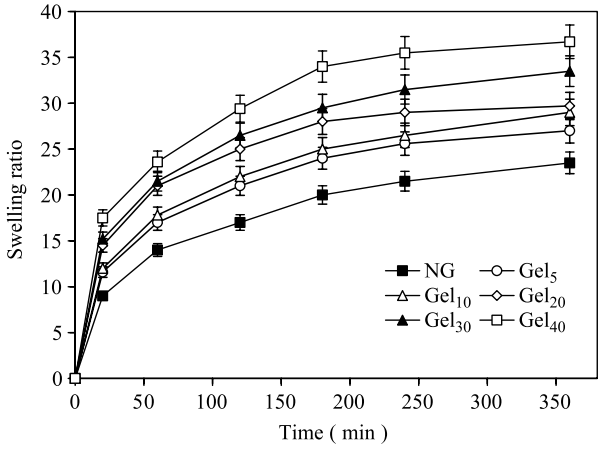

Fig. 8. Swelling kinetics of the freeze-dried, microgel-impregnated PNIPAAm hydrogels at 22 °C.

chemical similar and were prepared in the same fashion (i.e. pure water at room temperature). The second factor affecting the response rate is the extent of the special interactions among the polymers and binary solvents. Since there is no binary solvent used in the current study, we would expect there was no special interactions that could led to the formation of ternary complexes in the microgel impregnated hydrogels.

The third factor that could affect response rate is the characteristics of water release channels. For achieving quickly and timely diffusion of freed water during the shrinking at temperature above LCST, the hydrogel should have good release channels throughout the network. Thus, the most possible reason that the microgel-impregnated hydrogels exhibit faster response rate is attributed to the improved water release channels throughout the network in order to make water diffusing out quickly and timely during the deswelling process.

It is well-known that, during the shrinking course of PNIPAAm hydrogels at a temperature above LCST, the outermost surface of the hydrogel would be the first region to be affected. It is highly possible that the collapsed outermost surface layer is denser than the interior bulk matrix during the early stage of hydrogel shrinking process. Due to hydrophobic interaction between polymer chains, this layer would be thick and dense enough to restrict the outward permeation of entrapped water from the hydrogel interior, which greatly slows down the outflow rate of water [31–33]. Using a conventional pore-forming agent, such as PEG, could generate a macroporous PNIPAAm network and the formation of such a dense skin layer during the deswelling process could be avoided because the large pores cannot be collapsed tightly. Thus, water release channels would be kept open for the freed water to transfer out quickly [15]. However, a further increase in pore size of PNIPAAm hydrogels might impede the response rate because of some other factors, including the surface area as Zhuo et al. reported [17]. This suggests that large pore size alone is not the sole reason for the improved response rate.

In our previous investigations [29,33], it was found that increased pore number can achieve faster response rate too because more pores might provide more water release channels during the shrinking process. Compared with the morphological structure of NG, the increased numbers of pores in microgel-impregnated hydrogels (Gel_5–Gel_{40}, Fig. 1) may result in enhanced water release channels during the deswelling process. Therefore, the freed-water in microgel-impregnated hydrogels could diffuse out quickly at a temperature above their LCST. Other possible effect of the impregnated microgels on accelerated deswelling kinetics may be attributed to a more even heat and mass transfers within the microgel-impregnated PNIPAAm hydrogels because the volume occupied by the microgels had the similar chemical and thermo-responsive characteristics as the surrounding PNIPAAm matrix and hence there

was no discontinuity in structural characteristics, i.e. heat transfers from outside hot water to the innermost hydrogel matrix would occur rapidly, which could also result in a rapid phase separation throughout the matrix. In all, due to above reasons, the microgel impregnated hydrogels exhibit fast shrinking rate at temperatures above LCST and the response rate is accelerated from NG to Gel_5 to Gel_{40} with increasing microgel amounts.

3.6. Swelling kinetics

From the data in Fig. 8, it was found that the swelling rates of microgel-impregnated PNIPAAm hydrogels at room temperature were also improved when comparing to normal PNIPAAm hydrogel. During this hydration process, water penetration is a crucial step to determine the swelling kinetics of hydrogels. In the case of NG, its hydration was slower from the beginning of swelling process (smaller slop). NG absorbed about 9% water within 20 min, about 17% within 120 min and 23% at the end of 360 min. However, Gel_5 and Gel_{40} absorbed about 12 and 18% water within 20 min, respectively, and about 27 and 37% within 360 min, respectively. Among the microgel-impregnated PNIPAAm hydrogels, their swelling rates improve with an increase in microgel amounts as from Gel_5 to Gel_{40}.

Generally, three steps were suggested to control hydrogel swelling rate [33–35]: the diffusion of water molecules into hydrogel network, the subsequent relaxation of hydrated polymer chains, and the expansion of polymer network into surrounding aqueous solution. Therefore, porous morphology and nature of the pore cell wall are very important during the swelling process. This is because a porous morphology could increase the diffusion of water molecules into hydrogel network, while a thick and rigid pore cell wall would retard the relaxation of hydrated polymer chains. In reality, the swelling rate was the macroscopic observation resulted from the combination of these three steps. Based on the SEM observations in Fig. 1, the microgel-impregnated PNIPAAm hydrogels would exhibit a faster swelling rate than the normal one due to their increased pore number in microstructure and thinner cell wall.

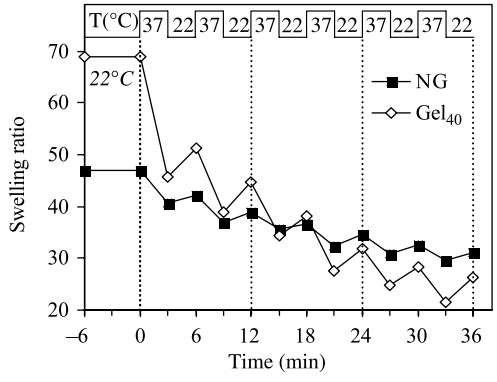

Fig. 9. Oscillatory shrinking–swelling kinetics of microgel-impregnated PNIPAAm hydrogels over 6-min temperature cycles in distilled water between 22 and 37 °C.

3.7. Oscillatory shrinking–swelling kinetics

The oscillatory shrinking–swelling kinetics of normal and microgel-impregnated PNIPAAm hydrogels were investigated over the 6-min temperature cycle between 22 (<LCST) and 37 °C (>LCST) in distilled water up to six cycles, and the data are shown in Fig. 9. The data show that both normal (NG) and microgel-impregnated (Gel_{40}) hydrogels exhibited an oscillatory shrinking–swelling character upon cycling temperature between 22 and 37 °C, accompanying with a consecutive reduction in the magnitude of swelling ratio due to their relatively slow reswelling rate when compared with their shrinking rate. When compared to NG, Gel_{40} exhibited much rapid, sharper and larger magnitude shrinking–swelling changes.

After the first cycle, the reduction in swelling ratio of Gel_{40} was around 9.5 ± 2.5 for each 3-min deswelling process at 37 °C and the increment in reswelling ratio was around 4.5 ± 1.0 for each 3-min reswelling process at 22 °C; where the corresponding data for NG were considerably smaller, 3.9 ± 0.9 and 1.6 ± 0.5, respectively. That is, the deswelling magnitude of Gel_{40} in the deswelling–swelling cycle was about 2.4 times that of NG, whereas the reswelling magnitude of Gel_{40} in the cycle was about 2.8 times that of NG.

This faster and larger magnitude of oscillating responses from microgel-impregnated PNIPAAm hydrogel may be advantageous for practical applications in fields such as bioengineering and biotechnology because faster response kinetics of the oscillating shrinking–swelling property of hydrogels to small temperature cycles (e.g. cycled around the physiological temperature) should be useful. On the other hands, the slower and smaller magnitude of the oscillatory action of NG, however, would limit its potential applications in such areas like the on–off switches for controlled drug release.

4. Summary

In summary, a new spherically-shaped PNIPAAm/PEG-DA microgel was used as an additive during the polymerization and gelation process of PNIPAAm hydrogels at room temperature for the purpose of improving thermosensitive property of PNIPAAm hydrogels without the expense of their mechanical property. The microgel-impregnated PNIPAAm hydrogels exhibited a tighter and more constrained porous network than pure PNIPAAm hydrogels without microgel additives. The pore size of the microgel-impregnated PNIPAAm hydrogels was reduced with an increase in the amounts of impregnated microgel. The presence of microgels within PNIPAAm hydrogels was evident by the appearance of spherical-shaped impression.

Due to the constrained and tighter network and increased polymer mass per unit volume, the mechanical property of microgel-impregnated PNIPAAm hydrogels were significantly higher than pure PNIPAAm hydrogels. Compared to a normal PNIPAAm hydrogel, LCSTs of the microgel-impregnated PNIPAAm hydrogels, however, did not change because of the same chemical nature between the microgels and their surrounding PNIPAAm matrix. The microgel additives greatly improved the thermosensitive property of PNIPAAm hydrogels in terms of swelling ratio, shrinking rate, swelling rate as well as the oscillatory shrinking–swelling kinetics upon temperature changes around LCST, and the level of improvement depended on the amounts of the microgel impregnated. Such improvements in mechanical and thermosensitive properties in the microgel-impregnated PNIPAAm hydrogels may find applications in biomedical and biotechnology fields.

Acknowledgements

We are grateful for the financial support of the National Textile Center, USA (Project No.: M01-CR01).

References

[1] Chen GH, Hoffman AS. Nature 1995;373:49–52.
[2] Liu ZS, Calvert P. Adv Mater 2000;12:288–91.
[3] Miyata T, Asami N, Uragami T. Nature 1999;399:766–9.
[4] Juodkazis S, Mukai N, Wakaki R, Yamaguchi A, Matsuo S, Misawa H. Nature 2000;408:178–81.
[5] Hirokawa Y, Tanaka T. J Chem Phys 1984;81:6379–80.
[6] Inomata H, Wada N, Yagi Y, Goto S, Saito S. Polymer 1995;36:875–7.
[7] Ramkissoon-Ganorkar C, Liu F, Baudyš M, Kim SW. J Controlled Release 1999;59:287–98.
[8] Stayton PS, Shimoboji T, Long C, Chilkoti A, Chen G, Harris JM, et al. Nature 1995;378:472–4.
[9] Liu F, Tao GL, Zhuo RX. Polym J 1993;25:561–7.
[10] Bae YH, Okano T, Hsu R, Kim SW. Makromol Chem Rapid Commun 1987;8:481–5.
[11] Osada Y, Okuzaki H, Hori H. Nature 1992;355:242–4.
[12] Hoffmann J, Plötner M, Kuckling D, Fischer WJ. Sens Actuators, A Phys 1999;77:139–44.
[13] Kon M, de Visser AC. Plast Reconstr Surg 1981;67:289–93.
[14] Oxley HR, Corkhill PH, Fitton JH, Tighe BJ. Biomaterials 1993;14:1064–72.
[15] Wu XS, Hoffman AS, Yager P. J Polym Sci, Part A: Polym Chem 1992;30:2121–9.
[16] Zhang XZ, Yang YY, Chung TS, Ma KX. Langmuir 2001;17:6094–9.
[17] Zhuo RX, Li W. J Polym Sci, Part A: Polym Chem 2003;41:152–9.
[18] Lin JK, Ladisch MR, Patterson JA, Noller CH. Biotechnol Bioeng 1987;29:976–81.
[19] Cai W, Gupta RB. J Appl Polym Sci 2002;83:169–78.
[20] Zhang XZ, Chu CC. Colloid Polym Sci 2004;282:1415–20.
[21] Zhang XZ, Chu CC. Am J Drug Deliv 2005;3:1–11.
[22] Cruise GM, Scharp DS, Hubbell JA. Biomaterials 1998;19:1287–94.
[23] Lin JK, Ladisch MR, Patterson JA, Noller CH. Biotechnol Bioeng 1987;29:976–81.
[24] Zhang XZ, Yang YY, Chung TS. J Colloid Interface Sci 2002;246:105–11.
[25] Zhang XZ, Chu CC. J Appl Polym Sci 2003;89:1935–41.
[26] Bae YH, Okano T, Kim SW. J Polym Sci, Part B: Polym Phys 1990;28:923–36.
[27] Inomata H, Goto S, Saito S. Macromolecules 1990;23:4887–8.
[28] Tokuhiro T, Amiya T, Mamada A, Tanaka T. Macromolecules 1991;24:2936–43.
[29] Zhang XZ, Wu DQ, Chu CC. J Polym Sci, Part B: Polym Phys 2003;41:582–93.
[30] Zhang XZ, Chu CC. Colloid Polym Sci 2004;282:589–95.
[31] Matsuo ES, Tanaka T. J Chem Phys 1988;89:1695–703.
[32] Yoshida R, Sakai K, Okano T, Sakurai Y. J Biomater Sci, Polym Ed 1992;3:243–52.
[33] Zhang XZ, Zhuo RX. J Colloid Interface Sci 2000;223:311–3.
[34] Yoshida R, Okuyama Y, Sakai K, Okano T, Sakurai Y. J Membr Sci 1994;89:267–77.
[35] Enscore DJ, Hopfenberg HB, Stannett VT. Polymer 1977;18:793–800.